A Micromachining Process for Die-Scale Pattern Transfer in Ceramics and Its Application to Bulk Piezoelectric Actuators

Tao Li and Yogesh B. Gianchandani, *Senior Member, IEEE*

***Abstract*—This paper reports on a batch mode planar pattern transfer process for bulk ceramics, glass, and other hard, brittle, nonconductive materials suitable for micromachined transducers and packages. The process is named LEEDUS, as it combines lithography, electroplating, batch mode micro electro-discharge machining (μEDM) and batch mode micro ultrasonic machining (μUSM). An electroplating mold is first created on a silicon or metal wafer using standard lithography, then using the electroplated pattern as an electrode to μEDM a hard metal (stainless steel or WC/Co) tool, which is finally used in the μUSM of the ceramic substrate. A related process (SEDUS) uses serial μEDM and omits lithography for rapid prototyping of simple patterns. Feature sizes of 25 μm within a 4.5×4.5 mm^2 die have been micromachined on glass-mica (Macor) ceramic plates with 34 μm depth. The ultrasonic step achieves 18 μm/min. machining rate, with a tool wear ratio of less than 6% for the stainless steel microtool. Other process characteristics are also described. As a demonstration, octagonal and circular spiral shaped in-plane actuators were fabricated from bulk lead zirconate titanate (PZT) plate using the LEEDUS/SEDUS process. A device of 20 μm thickness and 450 μm $\times$ 420 μm footprint produces a displacement of $\approx 2\mu$m at 40 V. [1652]**

***Index Terms*—Ceramic micromachining, microelectro-discharge machining (EDM), piezoelectric micro actuator, ultrasonic micromachining.**

I. Introduction

CERAMICS have been playing increasingly important roles in micromachined transducers and electronic applications [1]–[3]. Several types of ceramics have found applications in electronic and microelectromechanical systems (MEMS) packaging areas [4]–[6]. In addition to conventional semiconductor devices and IC high-performance packaging, ceramics are also attractive for microsystem packaging, such as for hermetic packages made entirely of ceramic or combination of ceramic and metals [7], [8]. In many of these cases, holes, grooves or complex patterns are often required on the ceramic substrates. As an important category of ceramics, piezoelectric ceramic materials, such as lead zirconate titanate (PZT) and related ferroelectric materials have been widely used in the fabrication of sensors and actuators [1], and PZT is of particular interest for MEMS applications due to its high piezoelectric coefficients and good electromechanical coupling [9].

Ceramics have their unique electrical, chemical, mechanical, and physical properties. Typically, they are hard, electrically and thermally insulating with high melting temperatures and high chemical stability. However, they are also brittle, with low toughness and ductility [7]. Although superb for packaging and device applications, these properties of ceramics also make them difficult to process lithographically. Consequently, ceramics (including PZT) are often processed by molding from a powder form, like dry pressing or tape casting, fused deposition (FDC) and sol gel process, etc. These additive processes, especially at micro level, can suffer from volume shrinkage, high temperature steps, nonuniform material properties and difficulty in mold forming. Thus, it is often desirable to directly pattern a bulk material without degrading the original material properties. However, subtractive processes have their own challenges. Serial subtractive processes like laser drilling and diamond grinding, which are most commonly used for conventional precision machining of ceramics, are unfavorable for complex patterns which can be best defined by a mask, with laser drilling also causing thermal shock and changes in morphology. For lithography based processes, reactive ion etching (RIE) is limited by a slow etch rate and varying gas requirements for different ceramics [10]. Phosphoric acid or other wet chemical etching methods for ceramics typically have limited etching rates and the achievable minimum feature size suffers due to lateral undercutting [11], [12]. For these reasons, RIE and wet etching are usually only used for patterning PZT thin films. Powder blasting provides good machining rates, but is limited by V-shaped sidewalls and blast lag [13], [14]. A bulk machining process with pattern-transfer capability continues to be a challenge.

Conventional ultrasonic machining (USM) has been widely accepted as an effective machining process for hard and brittle materials like ceramics, glass, etc. As these materials are brittle, it is easier to fracture them than to plastically deform them, and USM produces little or no damage or high-stress deformation at or below the surface. Moreover, it causes no thermal or chemical alterations in the subll prosurface characteristics of the machined material [15]. However, ultrasonic machining at micro level has only been utilized in nonlithographic ways, limiting both throughput and structural shapes [16], [17]. The batch mode micro ultrasonic machining (μUSM) approach presented in this paper facilitates die-scale transfer of complex lithographic patterns and provides relatively high resolution

Manuscript received July 9, 2005; revised December 5, 2005. This work was supported primarily by the Engineering Research Centers Program of the National Science Foundation under Award EEC-9986,866. Subject Editor E. Obermeier.

The authors are with the Engineering Research Center for Wireless Integrated Microsystems, University of Michigan, Ann Arbor, MI 48109-2122 USA (e-mail: litz@umich.edu).

Digital Object Identifier 10.1109/JMEMS.2006.876667

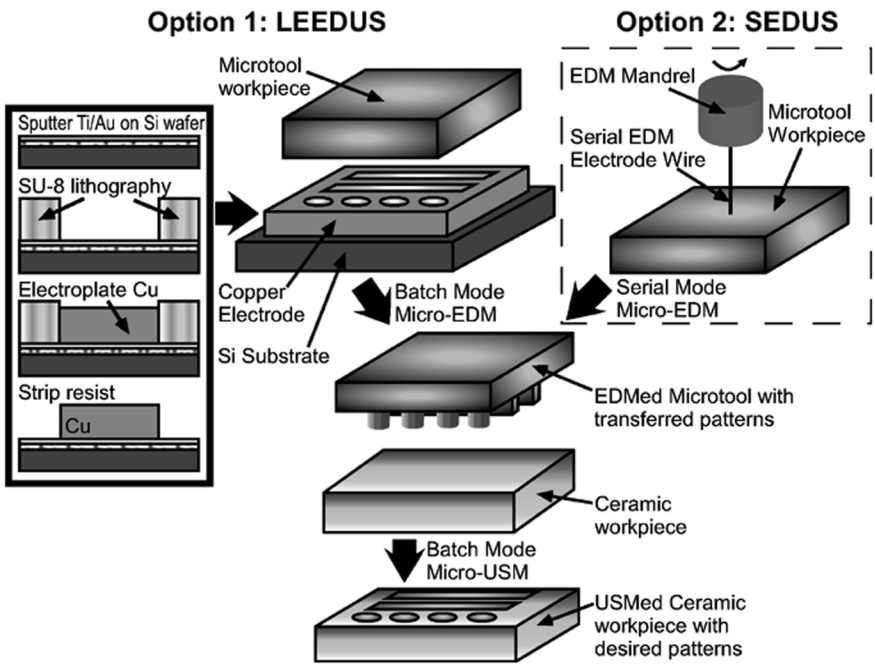

Fig. 1. LEEDUS process utilizes lithography, electroplating, and batch-mode μEDM to fabricate a microtool with a pattern which is defined by a mask, and then use batch-mode μUSM to transfer the pattern onto ceramic or other brittle materials. Nonlithographic rapid-prototyping can also be performed for simple patterns using option 2 (SEDUS).

and throughput, while retaining the favored characteristics of conventional USM.

In this paper, we present a fabrication process called LEEDUS,[1] which utilizes μUSM in batch mode to transfer a mask-defined die-scale pattern from a micro electro-discharge machined (μEDM'ed) microtool into a ceramic (including PZT) plate with high resolution and throughput. Microtools made from steel and WC/Co super hard alloy were explored. Section II gives details of the process flow and the setup created for batch mode μUSM. Section III discusses the results of the process characterization experiments. Octagonal and circular spiral in-plane actuators were fabricated from bulk PZT-5H plate using this process as a demonstration, and are described in Section IV.

II. Process Description

The LEEDUS process flow is illustrated in Fig. 1. A copper structure is electroplated into an SU-8 mold on a silicon substrate using a lithographically defined image of the final pattern. An alternative for this step is the LIGA process, which has the capability of mass production of ultra fine patterned high-aspect-ratio micro structures with very smooth side-wall surfaces [20], and may be more appropriate to fabricate the copper pattern when an aspect ratio greater than $10:1$ is required. The copper pattern on the silicon die is then used as an electrode to perform batch mode μEDM on a hard-metal microtool workpiece, transferring the corresponding negative die-scale pattern onto it [21], [22]. The setup used for batch mode μEDM is based on the Panasonic μEDM machine MG-ED72W. During the machining, electric discharges are fired between the electrode and the workpiece when they are both immersed in dielectric oil. This wears away both of them, but the workpiece is eroded much faster. By using lithographically defined electrodes, the batch mode μEDM can provide high throughput, high density and high uniformity over the whole array on any conductive materials. Finally the microtool is mounted on an ultrasonic machining setup for batch mode μUSM of a ceramic workpiece, thus having the desired positive pattern transferred onto it. Nonlithographic rapid-prototyping can also be performed for simple patterns by a similar process, in which the original serial μEDM function of the MG-ED72W machine is used to define the pattern on the microtool by running a program on a computer to control the "writing" movement of the rotating EDM electrode wire on the microtool workpiece. This derivative of the process is called SEDUS (serial electro-discharge and ultrasonic machining).

The schematic diagram for the setup built for batch mode μUSM is shown in Fig. 2. This setup has a manually controlled X-Y stage for relative positioning of the microtool and the ceramic workpiece. The Z stage is motorized and computer-controllable. A force sensor is implemented on the Z stage to monitor the machining load and provide feedback signal when necessary, so that the setup can work in either a constant machining load mode or a constant feeding speed mode. The vibration amplitude of the ultrasonic transducer is adjustable down to 20% of the full scale output. The μEDM'ed microtool is mounted by epoxy at the tip of the horn where the vibration energy generated by the ultrasonic transducer is maximized in the vertical direction. Abrasive slurry which consists of water and fine abrasive powders is supplied between the tip of the microtool and a ceramic workpiece. The vibrating tip of the microtool is fed into the ceramic workpiece. The ultrasonic motion of the microtool imparts velocity to the abrasive particles on its downward

[1]Portions of this paper have been presented in conference abstract form in [18] and [19].

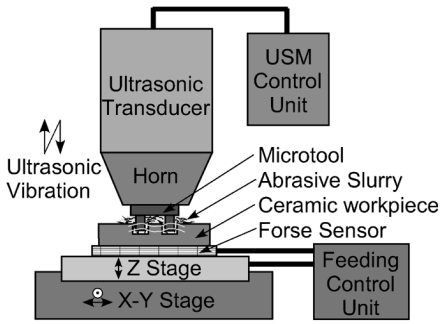

Fig. 2. μUSM setup created for batch mode pattern transfer to ceramic workpiece.

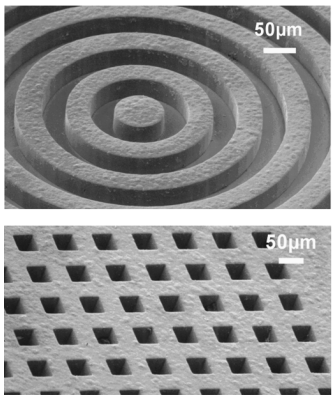

Fig. 3. SEM photos of two of the patterns on electroplated copper die (both with 40 μm feature size).

stroke. These particles, in turn, are responsible for the erosion of the workpiece, thus creating the desired cavities in the shape of the microtool.

III. Process Characterization

A set of experiments were performed to characterize the process. A 4.5 mm $\times$ 4.5 mm silicon die with 50 μm high electroplated copper structures on top of Ti/Au adhesion layer was used as the electrode for batch mode μEDM of stainless steel or WC/Co microtools. The EDM discharge voltage was 80 V and the discharge control capacitance was 100 pF. Fig. 3 shows SEM images of two of the demonstrative copper patterns, both of which have features with lateral dimension of 40 μm. Fig. 4 shows μEDM'ed microtools made with stainless steel and WC/Co. The grainy nature of WC/Co led to a rougher finish. The 40 μm features in the copper pattern were reduced to 24 μm on the microtool due to the μEDM discharge gap which was measured as about 8 μm. This gap is generally determined by the discharge energy and is stable under fixed discharge conditions when the secondary EDM discharge caused by machining debris is minimized. The dimension of the electrode patterns should be designed while keeping this gap in mind.

The stainless steel microtool was then used for batch mode μUSM on a glass-mica (Macor) ceramic plate whose properties are listed in Table I. The ultrasonic vibration utilized for the demonstration had a frequency of 20 KHz and amplitude of 15 μm. The abrasive was WC powder in water with particle size of 0.5–1 μm. Results are shown in Fig. 5. A minimum feature size

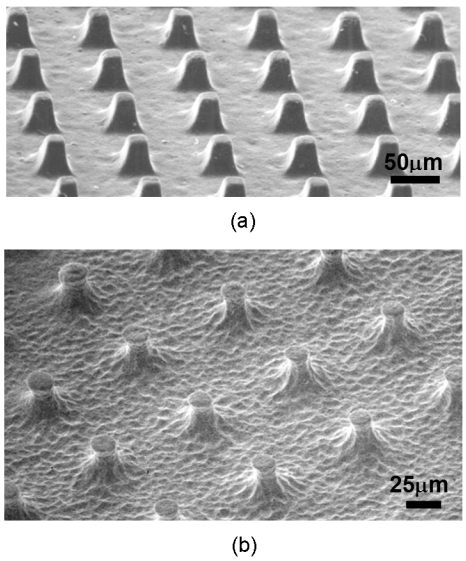

Fig. 4. SEM photos of batch mode μEDM'ed microtools. (a) Stainless steel microtool pattern of 35 μm height. (b) WC/Co microtool pattern of 32 μm height.

TABLE I
Material Properties for the Ultra-High Temperature Glass-Mica (Macor) Ceramic Plate Used in the Experiments (Quoted From McMaster Carr. Item No. 8489K231)

Temperature Range	-185°C to 800°C
Flexural Strength	94 MPa
Compressive Strength	345 MPa
Dielectric Strength	3.94×10^{7} volt/m
Thermal Conductivity	1.46 W/m•K
Density	2.5×10^{3} Kg/m^{3}
Others	Nonporous, opaque white

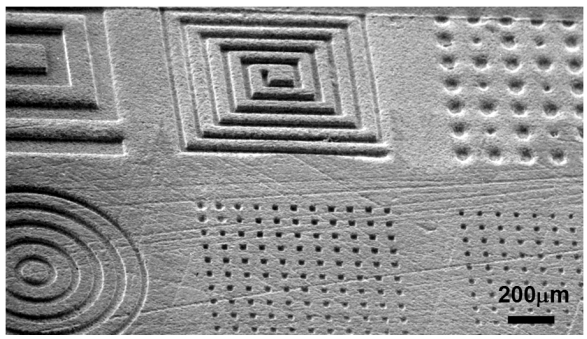

Fig. 5. SEM photo of patterns on the Macor ceramic plate transferred from the die-scale stainless steel microtool. The scouring on the surface was present in the unprocessed workpiece. It is notable that the pattern transfer does not remove it.

of 25 μm on the ceramic plate was achieved with a machining depth of 34 μm. The overall process performance achieved is summarized in Table II.

The average machining rate observed in this demonstration was 18 μm/min, with ≈ 5 mm^{2} cutting surface area and ≈ 0.5 N machining load. For USM, the machining rate usually increases with any of the following: The brittle fracture hardness of the workpiece material, mean radius of abrasive grains, working load applied in the cutting zone, amplitude of vibration, and frequency of oscillation [23]. Fig. 6 shows the change of machining

TABLE II
MACHINING PARAMETERS FOR THE BATCH MODE μUSM OF THE MACOR CERAMIC PLATE

Transducer frequency	20 KHz
Vibration amplitude	15 μm
Abrasive powders	WC (0.5 to 1 μm)
Batch machining die area	4.5 mm × 4.5 mm
Avg. machining rate	18 μm/min.
Machining load	≈0.5 N
Minimum feature size	25 μm
Cutting depth	34 μm
Surface roughness measured pre / post processing (Ra)	≈0.55 μm / 0.4 μm
Tool wear ratio(height)	< 6% (Stainless steel)

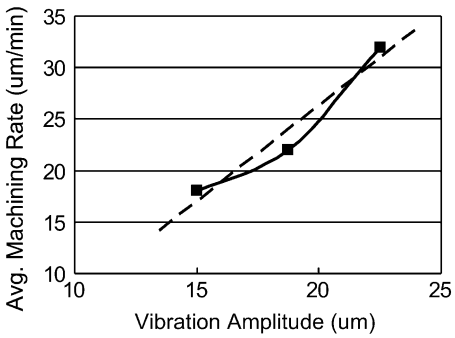

Fig. 6. Variation of machining rate as the amplitude of ultrasonic vibration is increased (Other machining parameters remain the same as those in the characterizing test).

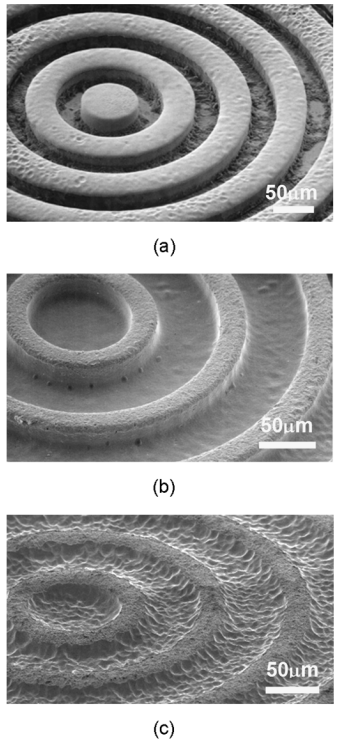

Fig. 7. Post-use SEM photos. (a) Copper electrode used after μEDM of the steel microtool, tool wear ratio $\approx 29\%$. (b) Stainless steel microtool, after μUSM of the ceramic part, tool wear ratio $<6\%$. (c) WC/Co microtool, after μUSM of the ceramic part, tool wear ratio $>25\%$.

rate with increasing amplitude of ultrasonic vibration. A linear relationship was assumed for the dashed trend line. Although larger amplitude results in faster machining speed, the surface finish becomes rougher and chips at feature edges can occur.

Fig. 7(a) shows the copper electrode after μEDM of the stainless steel microtool. A tool wear ratio of $\approx 29\%$ was measured, which corresponds to ≈ 10 μm loss of copper tool height for making a 35 μm high microtool. This tool wear can be compensated by increasing the SU-8 mold height or using LIGA process to get a higher copper electrode, or can be reduced using parallel discharge mode μEDM with partitioned die area as described in [21]. The machining debris, which is prone to get clogged in the array when the die area is large, also contributes to the large tool wear. An approach to facilitate debris removal during machining would be much preferred to minimize this tool wear.

The wear ratio of μUSM microtools usually varies with different tool materials, or changes with machining parameters such as machining load, abrasive powder size, etc. In order to compare microtool materials, the WC/Co microtool was also tested for μUSM under the same machining parameters. Fig. 7(b) and (c) show post-use stainless steel and WC/Co microtools respectively. The stainless steel microtool gave a wear ratio of $<6\%$, taking as the ratio of tool height worn vs. cutting depth, while the WC/Co microtool showed a wear ratio of $\approx 4\times$ higher, likely due to its brittleness which is a preferred characteristic for USM. This suggests stainless steel is a better choice for this application, opposing the usual preference for WC/Co as a machining tool material.

Fig. 8(b) shows the hole width distribution for the 9×9 array of 35 μm features in Fig. 8(a). The average hole width is 34.8 μm. The standard deviation of holes sizes is 0.88 μm, providing acceptable size uniformity for many applications.

IV. DEVICE FABRICATION AND TESTING

Piezoelectric ceramics such as PZT are nowadays widely used for sensing or actuating applications. For PZT materials, both the piezoelectric longitudinal d_{33} and transverse d_{31} coefficients are often used. When the longitudinal coefficient d_{33} is applied directly for actuating ($\Delta h = d_{33} \cdot V$), a high voltage ($>1$ KV) is required to generate a reasonable displacement (e.g., 1 μm) due to the relatively low d_{33} value of the materials. Although d_{31} is even less than 50% of d_{33}, the transverse displacement ($\Delta h = L/W \cdot d_{31} \cdot V$) can be much higher by a factor of length-to-width (L/W) aspect ratio than the longitudinal displacement of a sufficiently long PZT beam actuator, where V is the actuating voltage, Δh is the resulting displacement. For example, with a normal d_{31} value of -300 pm/V, a 1 μm displacement can be generated under 50 V actuating voltage if the straight beam actuator has an aspect ratio of >67.

By transforming the straight beam with large aspect ratio into a plane coil with spiral geometry, the total size of the actuator can be significantly reduced. It has been shown in macro-scale that a spiral shape PZT actuator of 3-cm diameter with metallized sidewall electrodes can provide in-plane displacement at the tip of the spiral which is $5\text{–}12\times$ larger than that of an equivalent straight beam actuator with the same effective length of 26 cm [24], [25]. Some other spiral PZT actuators are described in [26], [27]. All these results were achieved exclusively

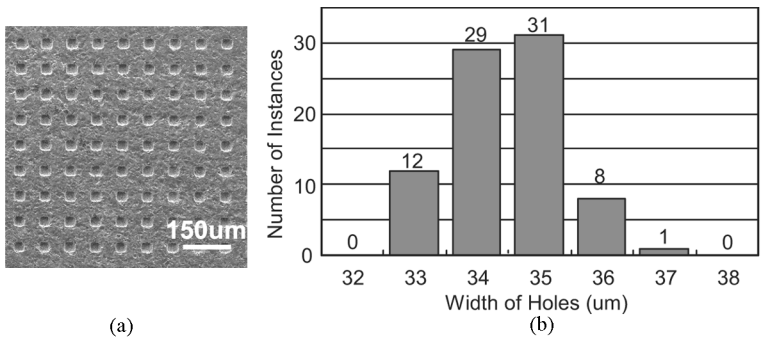

Fig. 8. (a) SEM photo of an 81-hole array of 35 μm-width holes transferred from WC/Co microtool. (b) Size variation in the array. Mean holes width: 34.8 μm. Standard deviation: 0.88 μm.

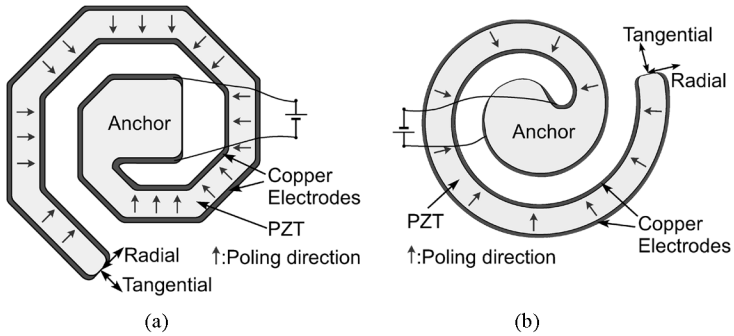

Fig. 9. Schematic of (a) octagonal spiral actuator and (b) circular spiral actuator. The short arrows indicate poling direction along the spiral.

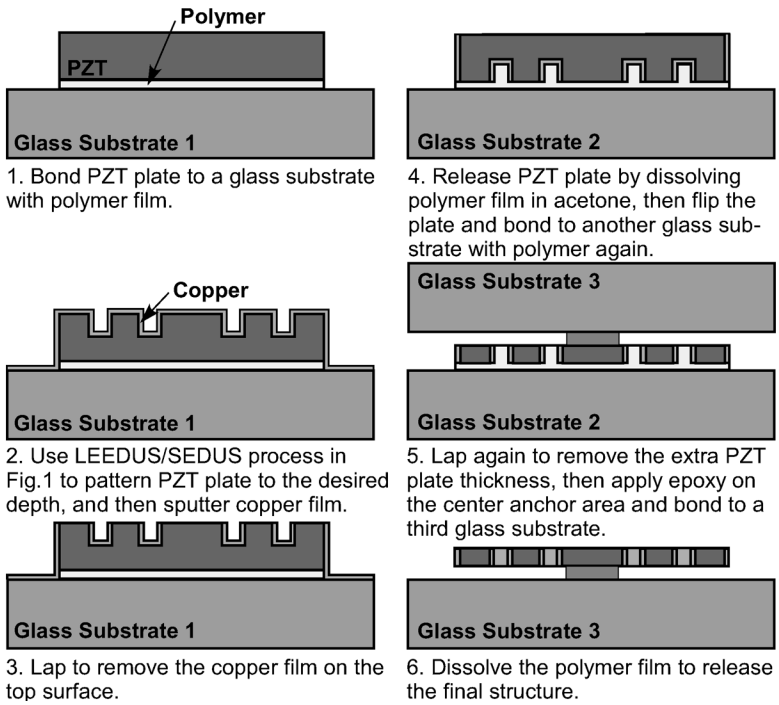

Fig. 10. In-plane PZT actuator fabrication process flow.

using additive fabrication processes, because unlike ultrasonic machining, traditional machine cutting process would result in microcracks and structural damage on the brittle PZT material. Neither has micromachining result ever been reported on the spiral PZT actuators.

These spiral shape actuators were chosen to demonstrate the practical use of the LEEDUS/SEDUS process. Both octagonal and circular spiral geometries were designed as shown in Fig. 9. Note that the circular version is only possible with LEEDUS process due to the machining limitation of serial mode μEDM in SEDUS process. As shown in Fig. 10, the fabrication starts with a bulk PZT-5H plate with excellent material properties for actuating. The PZT plate is bonded to a glass substrate. Either LEEDUS or SEDUS process is carried out to get the desired

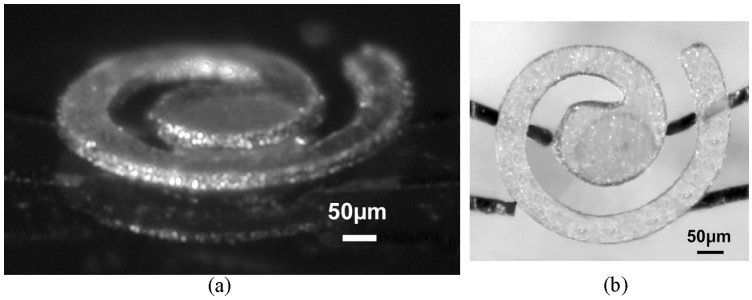

Fig. 11. Photos with perspective and topdown view of the final released circular spiral actuator supported on its center anchor with epoxy. This device was fabricated by LEEDUS using the design shown in Fig. 9(b).

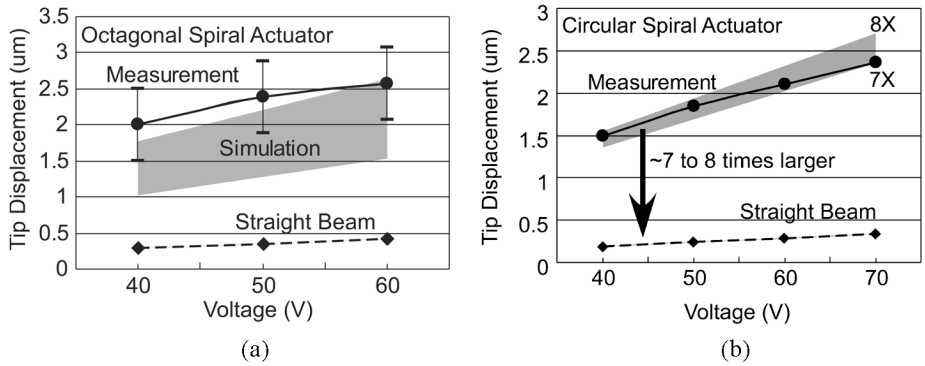

Fig. 12. Measured displacement at the tip of the spirals as a function of actuating voltages, compared with the calculated d_{31} transverse displacement of corresponding PZT-5H straight beam actuators with the same effective length. (a) Octagonal spiral results (Effective length $= 1101\,\mu$m, Width $= 49.7\,\mu$m, $d_{31} = -320$ pm/V). FEMLAB simulation result (shaded area) is shown as a range, caused by uncertainty in the material properties and device geometry nonideality. An estimated measurement error of $\pm 0.5\,\mu$m is indicated by error bar for the measurement results. (b) Circular spiral results (Effective length $= 1205\,\mu$m, Width $= 79.5\,\mu$m, $d_{31} = -320$ pm/V). Shaded area indicates the corresponding multiples (7× to 8×) of displacement of the straight beam actuator.

pattern on the PZT plate, and then Cu/Ti film is sputtered. The copper film on the top surface is removed by lapping, and then the PZT plate is flipped by releasing in acetone and bonding again to a second glass substrate. Lapping is carried out again to remove the extra thickness of the PZT plate, and epoxy is applied at center anchor area to bond the structure to a third glass substrate. Finally, the device is released and in-situ poling is carried out.

The μEDM'ed microtools for both the octagonal and the circular spiral actuators were machined using stainless steel. The octagonal spiral microtool made by serial μEDM had a cutting depth of 100 μm and can be easily adjusted by modifying the controlling program. The circular spiral made by batch μEDM had a cutting depth of 48 μm. The final released device supported at the center anchor by epoxy is shown in Fig. 11 for the circular version. The octagonal spiral actuator has a footprint of 450 μm × 420 μm, beam width of 50 μm and height of 20 μm, and the circular one has an outer diameter of 500 μm, beam width of 80 μm and height of 28 μm. These devices were poled *in-situ* by a bias to the copper electrodes on their sidewalls using a probe station.

The testing results of the actuators displacement are shown in Fig. 12. For the octagonal spiral actuator, a displacement of $\approx 2\,\mu$m was achieved at an actuating voltage of 40 V, and this measured displacement is 6–7 × larger than the calculated d_{31} transverse displacement from an equivalent straight beam actuator. For the circular version, the multiple is 7–8 × , giving similar results as that shown in [24]. It is obvious that the transverse d_{31} effect is not the sole cause for the measured displacement. One explanation given in [24] is that the nonuniform stress developed under applied voltage creates a bending moment, which changes the curvature of the spiral and results in the magnified displacement at the tip. This magnification multiple is related to the effective length and wall width of the actuator as discussed in [24]. In both cases, the displacement started dropping at higher actuating voltage. This is likely due to a degradation of polarization when the applied electric field is too strong, reaching the initial depolarization field of ≈500–1000 V/mm.

A FEM analysis was performed for the octagonal spiral actuator using FEMLAB Multiphysics (now COMSOL Multiphysics) simulation software. In the simulation, Piezo Solid application mode was used for modeling. As poling was performed by applying voltage on the sidewall of the spiral beam, in order to model the varying polarization direction along the spiral beam as shown in Fig. 9(a), a local coordinate system was created for each segment of the octagonal spiral geometry. The geometry parameter and the manufacture's material properties for the PZT-5H bulk plate are summarized in Table III. To accommodate the device geometry nonideality and uncertainty in the PZT material properties caused by poling and estimation of some parameters, estimated variation of up to 15% of these parameters were used during simulation. The simulation results,

TABLE III
GEOMETRY PARAMETER AND MATERIAL PROPERTIES USED FOR FEM ANALYSIS. ERROR OR UNCERTAINTY ESTIMATION OF UP TO $\pm 15\%$ WAS ADDED TO THESE PARAMETERS DURING SIMULATION

Spiral beam width	50 μm
Spiral beam thickness	20 μm
PZT density	7800 Kg/m^3
Piezoelectric coefficient d_{31}	-320 pm/V
Piezoelectric coefficient d_{33}	650 pm/V
PZT relative permittivity K^T_3	3800
Elastic modulus Y^E_3	50 GPa
Elastic modulus Y^E_1	62 GPa

which are shown in Fig. 12(a) as shaded area, approximately matches to the measurement result although the variation of the simulation parameters caused a range of simulation results.

V. DISCUSSION

The μUSM technology included in this process has some advantages over the traditional methods when applied to hard, brittle materials, in that it does not degrade the workpiece material in terms of damage, stress regimes and thermal or chemical alterations. It can achieve precision surface finish of Ra 0.4–0.76 μm [15]. In traditional machining, the mechanism for removing material causes plastic deformation at the micro scale, resulting in microcracks and other damage in brittle materials. Another option for making microstructures is to use an additive process, i.e., one in which the structural material is selectively deposited onto a substrate. However, with these it is difficult to get the desired uniformity in terms of material properties.

The μUSM cutting rate demonstrated in this work is >18 μm/min. for both Macor and PZT, while RIE etching of PZT is at 0.3 μm/min. [10], and wet etching of PZT is at 0.13 μm/min. [12]. Powder blasting can reach an etching rate of 25 μm/min. for glass [13] and a minimum feature size of 30 μm [28], but it has the problems of V-shaped sidewalls and blast lag, which becomes rather severe when the feature size gets smaller and the cutting depth gets larger. For μUSM, the machined cavities follow the shape of the microtool, eliminating V-shaped sidewalls or blast lag problems. It can be seen that complex lithographic patterns, such as the circles and spirals in Figs. 7 and 9, present significant challenges for previously established methods. RIE and wet etching are too slow to be efficiently used for bulk micromachining of PZT, while the V-shaped sidewalls made by powder blasting will make it difficult to form electrodes on the sidewalls of these shapes.

The LEEDUS and SEDUS processes have been demonstrated at die-scale. An eventual target of wafer-scale pattern transfer would be beneficial to a number of applications in terms of throughput. However, there are still some limitations that prevent the process from going to wafer level. The batch mode μEDM used to make microtools presents the first major barrier. Although parallel discharge mode can be used to improve the scaling limit, the debris generated at the center of the wafer can cause secondary discharge and damage the electrodes. (This may also ultimately limit the aspect ratio achievable in LEEDUS.) New techniques for flushing debris are under investigation for a solution of the debris problem [29], [30]. Another limitation would come from the microtool mounting error, i.e., the error of the parallelism between the surfaces of the microtool and the workpiece during μUSM. If the machining area is increased to wafer level, this problem becomes much more significant than it is for die-scale machining. New mounting techniques or a compensation mechanism on the Z-stage would be necessary to reduce this error.

VI. CONCLUSION

A new fabrication process (LEEDUS) which combines lithography, electroplating, batch mode μEDM and batch mode μUSM, has been developed to provide die-scale pattern transfer capability from lithographic mask onto ceramics, including piezoceramics like PZT, PMN-PT, etc. A related process (SEDUS) uses serial μEDM and omits lithography for fast prototyping of simple patterns. A die-scale pattern with 25 μm minimum feature sizes was defined with a mask and transferred onto Macor ceramic workpieces by stainless steel and WC/Co microtools with a machining speed of 18 μm/min. As a demonstration, octagonal and circular spiral shaped in-plane actuators were fabricated from bulk PZT-5H plate. The octagonal spirals had a footprint of 450 μm $\times$ 420 μm and beam width of 50 μm, while the circular version had an outer diameter of 500 μm and beam width of 80 μm. Measurements showed that the displacement is 6–8 $\times$ larger than the calculated d_{31} transverse displacement from a straight beam actuator with the same equivalent length, indicating that practical devices can be made with this process. The experimental results are very promising for further improvements, and will be pursued in future efforts.

ACKNOWLEDGMENT

The authors are grateful to the Solid-State Electronics Laboratory (SSEL) colleagues at the University of Michigan, Ann Arbor, especially Dr. K. Takahata, Mr. W. Zhu, and Dr. K. Udeshi for their help with the equipment. The authors would also like to thank Prof. K. Najafi and Mr. J. Giachino at UM WIMS ERC for valuable discussions. Facilities used for this research include the Michigann Nanofabrication Facility (MNF) at the University of Michigan.

REFERENCES

[1] R. C. Buchanan, Ed., *Ceramic Materials for Electronics: Processing, Properties, and Applications*. New York, NY: Marcel Dekker, 1986.
[2] W. Y. Howng, "Ceramic technologies for portable radio applications," in *Materials and Processes for Wireless Communications, Ceramic Transactions*. Westerville, OH: American Ceramic Society, 1995, vol. 53.
[3] P. N. Kumta, G. S. Rohrer, and U. Balachandran, Eds., *Role of Ceramics in Advanced Electrochemical Systems, Ceramic Transactions*. Westerville, OH: American Ceramic Society, 1996, vol. 65.
[4] M. F. Yan, K. Niwa, H. M. O'Bryan, and W. S. Young, Eds., *Ceramic Substrates and Packages for Electronic Applications, Advances in Ceramics*. Westerville, OH: American Ceramic Society, 1987, vol. 26.
[5] D. W. Palmer, "High-temperature electronics packaging," in *High Temperature Electronics*, R. Kirschman, Ed. New York: IEEE Press, 1999.
[6] K. Otsuka, *Multilayer Ceramic Substrate-Technology for VLSI Package/Multichip Module*. London, U.K.: Elsevier Applied Science, 1993.
[7] W. D. Brown, Ed., *Advanced Electronic Packaging: With Emphasis on Multichip Modules*. New York: IEEE Press, 1999.
[8] S. Caplet, N. Sillon, M. T. Delaye, and P. Berruyer, "Vacuum wafer-level packaging for MEMS applications," *Proc. SPIE*, vol. 4979, pp. 271–278, 2003.

[9] S. Trolier-Mckinstry and P. Muralt, "Thin film piezoelectrics for MEMS," *J. Electroceramics*, vol. 12, no. 1–2, pp. 7–17, Jan.–Mar. 2004.
[10] S. Wang, X. Li, K. Wakabayashi, and M. Esashi, "Deep reactive ion etching of lead zirconate titanate using sulfur hexafluoride gas," *J. Amer. Ceramic Soc.*, vol. 82, no. 5, pp. 1339–41, May 1999.
[11] E. Makino, T. Shibata, and Y. Yamada, "Micromachining of fine ceramics by photolithography," *Sensors Actuators A (Phys.)*, vol. 75, no. 3, pp. 278–288, Jun. 1999.
[12] L.-P. Wang, R. Wolf, Q. Zhou, S. Trolier-McKinstry, and R. J. Davis, "Wet-etch patterning of lead zirconate titanate (PZT) thick films for microelectromechanical systems (MEMS) applications," in *Proc. Materials Science of MEMS Devices III. Symp.*, Boston, MA, 2000, pp. EE5.39.1–EE5.39.6.
[13] H. Wensink, J. W. Berenschot, H. V. Jansen, and M. C. Elwenspoek, "High resolution powder blast micromachining," in *Proc. IEEE Int. Conf. Microelectromechanical Systems (MEMS)*, 2000, pp. 769–774.
[14] M. Wakuda, Y. Yamauchi, and S. Kanzaki, "Material response to particle impact during abrasive jet machining of alumina ceramics," *J. Mater. Process. Tech.*, vol. 132, no. 1–3, pp. 177–183, Jan. 2003.
[15] T. B. Thoe, D. K. Aspinwall, and M. L. H. Wise, "Review on ultrasonic machining," *Int. J. Machine Tools Manuf.*, vol. 38, no. 4, pp. 239–255, Apr. 1998.
[16] X. Sun, T. Masuzawa, and M. Fujino, "Micro ultrasonic machining and its applications in MEMS," *Sensors Actuators A (Phys.)*, vol. A57, no. 2, pp. 159–64, Nov. 1996.
[17] H. Choi, S. Lee, and B. Lee, "Micro-hole machining using ultrasonic vibration," *Key Eng. Mater.*, vol. 238–239, pp. 29–34, 2003.
[18] T. Li and Y. B. Gianchandani, "LEEDUS: A micromachining process for die-scale pattern transfer in ceramics with high resolution and throughput," in *Proc. Solid State Sensor, Actuator and Microsystems Workshop (Hilton Head)*, Hilton Head Island, SC, Jun. 2004, pp. 324–327.
[19] T. Li and Y. B. Gianchandani, "A die-scale micromachining process for bulk PZT and its application to in-plane actuators," in *Proc. IEEE Int. Conf. Microelectromechanical Systems (MEMS 05)*, Miami Beach, FL, Jan. 2005, pp. 387–390.
[20] H. Guckel, "High-aspect-ratio micromachining via deep X-ray lithography," *Proc. IEEE*, vol. 86, no. 8, pp. 1586–93, Aug. 1998.
[21] K. Takahata and Y. B. Gianchandani, "Batch mode micro-electro-discharge machining," *IEEE/ASME J. Microelectromech. Syst.*, vol. 11, no. 2, pp. 102–110, Apr. 2002.
[22] K. Takahata, N. Shibaike, and H. Guckel, "High-aspect-ratio WC-Co microstructure produced by the combination of LIGA and micro-EDM," *Microsyst. Technol.*, vol. 6, no. 5, pp. 175–8, 2000.
[23] M. Komaraiah and P. N. Reddy, "A study on the influence of workpiece properties in ultrasonic machining," *Int. J. Machine Tools Manuf.*, vol. 33, no. 3, pp. 495–505, 1993.
[24] F. Mohammadi, A. L. Kholkin, B. Jadidian, and A. Safari, "High-displacement spiral piezoelectric actuators," *Appl. Phys. Lett.*, vol. 75, no. 16, pp. 2488–90, Oct. 1999.
[25] F. Mohammadi, B. Jadidian, A. L. Kholkin, S. C. Danforth, and A. Safari, "Electromechanical properties of piezoelectric spiral actuators," in *Proc. 2000 12th IEEE Int. Symp. Applications of Ferroelectrics (ISAF)*, Honolulu, HI, 2000, pp. 101–104.
[26] H. H. Kolm and E. A. Kolm, "Spiral piezoelectric rotary actuator," U.S. Patent no. 4 435 667, 1984.
[27] V. V. Lavrinenko, A. P. Miroshnichenko, and V. A. Khraschevsky, "Method of making piezoelectric element," U.S. Patent no. 3 781 955, 1974.
[28] H. Wensink and M. C. Elwenspoek, "Reduction of sidewall inclination and blast lag of powder blasted channels," *Sensors Actuators A (Phys.)*, vol. 102, pp. 157–164, 2002.
[29] M. T. Richardson and Y. B. Gianchandani, "A passivated electrode batch μEDM technology for bulk metal transducers and packages," in *Proc. IEEE Conf. Sensors*, Anaheim, CA, Nov. 2005, pp. 219–222.
[30] M. T. Richardson, Y. B. Gianchandani, and D. S. Skala, "A parametric study of dimensional tolerance and hydrodynamic debris removal in micro-electro-discharge machining," in *Proc. IEEE Int. Conf. Microelectromechanical Systems (MEMS 06)*, Istanbul, Turkey, Jan. 2006, pp. 314–317.

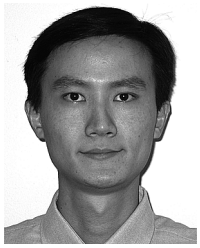

Tao Li received the B.S. and M.S. degrees in engineering from Tsinghua University, Beijing, China, in 2000 and 2002, respectively, with a major in precision instruments. He is currently working toward the Ph.D. degree in electrical engineering at the University of Michigan, Ann Arbor, with a focus in circuits and microsystems.

His research interests are in the area of nontraditional microfabrication technologies and their applications, combined with traditional silicon-based technologies, to MEMS devices and microsystems.

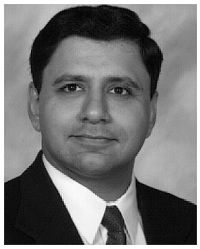

Yogesh B. Gianchandani (S'83–M'85–SM'04) received the B.S., M.S, and after some time in industry, Ph.D. degrees, all in electrical engineering, with a focus on microelectronics and MEMS.

He is currently an Associate Professor in the Electrical Engineering and Computer Science Department and holds a joint appointment in the Department of Mechanical Engineering at the University of Michigan, Ann Arbor. Prior to this, he was with the Electrical and Computer Engineering Department at the University of Wisconsin, Madison. He has also held industry positions with Xerox Corporation, Microchip Technology, and other companies, working in the area of integrated circuit design. His research interests include all aspects of design, fabrication, and packaging of micromachined sensors and actuators and their interface circuits. At the University of Michigan, Prof. Gianchandani serves as the Director of the College of Engineering Interdisciplinary Professional Degree Program in Integrated Microsystems.

Prof. Gianchandani is the recipient of a National Science Foundation Career Award, and he has published about 150 papers in the field of MEMS, and has about 25 patents issued or pending. Prof. Gianchandani serves on the editorial boards of *Sensors and Actuators, IOP Journal of Micromechanics and Microengineering*, and *Journal of Semiconductor Technology and Science*. He also served on the steering and technical program committees for the IEEE/ASME International Conference on Microelectromechanical Systems (MEMS) for many years, and served as a General Co-Chair for this meeting in 2002.